JOURNAL OF NANO- AND ELECTRONIC PHYSICS
Vol. **4** No 1, 01007(7pp) (2012)

ЖУРНАЛ НАНО- ТА ЕЛЕКТРОННОЇ ФІЗИКИ
Том **4** № 1, 01007(7cc) (2012)

The Role of Nano-sized Fraction on Spark Plasma Sintering the Pre-Alloyed Spark-Erosion Powders

G.E. Monastyrsky[1*], P. Ochin[2], A.V. Gilchuk[1], V.I. Kolomytsev[3], Yu.N. Koval[3]

[1] *NTUU "KPI", 37, Peremogy Av., UA-03506 Kyiv, Ukraine*
[2] *ICMPE-CNRS, 2-8, rue Henri Dunant-94320 Thiais, France*
[3] *IMP of NASU, 36, Vernadsky Av., UA-03142, Kyiv, Ukraine*

(Received 18 October 2011; revised manuscript received 22 February 2012; published online 14 March 2012)

Ti-Ni-Hf, Ni-Al and Cu-Al-Ni shape memory materials were produced by spark plasma sintering method from the micron and nano-sized particles prepared by spark-erosion method in cryogenic liquid from preliminary melted master alloys. The effects of spark plasma sintering processing parameters on the martensitic transformation and microstructure of the sintered compacts were investigated using XRD and SEM methods. Although precipitating processes were usually not completely depressed, the intensive grain growth was also not found in most cases. Most of the microstructure peculiarities of as processed powder were inherited by the sintered material. The contradictory role of the nano-sized fraction of powders is discussed: in most case this fraction promotes the rapid sintering but also the oxidation proceses in sintered compacts.

Keywords: Shape memory alloys, Spark-erosion powders, Spark plasma sintering, Ti-Ni, Ni-Al, Cu-Al-Ni.

PACS numbers: 81.05.Bx, 81.20.Ev, 81.30.Kf, 81.30.Mh

1. INTRODUCTION

Attractive perspectives of the practical application the materials with conventional and magnetic shape memory, high-temperature shape memory stimulate continuous searching new production and processing methods. The direction of searching is caused by their typical characteristics and requirements that are imposed to them. In most cases shape memory materials, high temperature shape memory materials have precise composition, some of them contain or highly reactive or high-cost components and moreover are a multicomponent. Thus the requirement to their compositions is especially important. Most of these materials tend to the decomposition during the heat treatment. In addition, they, with few exceptions, have poor ductility and machinability.

In this communication we will focus on three materials, which are representative most of above mentioned peculiarities of functional materials: Cu-Al-Ni-Ti-Cr, Ni-Al and Ti-Ni-Hf shape memory alloys (SMA). These kinds of SMA are being developed as ones of the alternatives for the intermediate and high temperature applications depending on the alloying content.

Cu-Al-Ni is considered as good candidate for the intermediate temperature applications (100-300 °C). In Cu-Al-Ni, during the quenching the metastable β phase undergoes several types of martensitic transformation (MT) depending on Al content. The characteristics of the martensitic transformation MT are very sensitive to the order degree of the β phase and the precipitation processes. Primary γ_1 precipitation limits the high temperature applications of these alloys modifying the MT. The eutectic decomposition takes place above 440 °C and finally the $\beta \rightarrow \alpha + \gamma_1$ eutectoid decomposition appears at 500 °C. Increasing Al content promotes the formation γ_1 phase that embrittles the alloy. In addition Cu-Al-Ni alloys are brittle due to their very high elastic anisotropy (A~13) and large grain size and in general show poor mechanical properties. Powder metallurgy is to be a good method in order to obtain finer grain size in Cu-Al-Ni SMA.

Enriched with Ni intermetallic Ni-Al is a promising shape memory alloy (SMA) for high-temperature applications with the start temperature of martensitic transformation between 200 and 1200 K depending on Ni content. Currently, its wide application is limited by low plasticity, in particular due to the formation of intermetallic compounds Ni_3Al and Ni_5Al_3 during the preparation or heat treatment. By means of the traditional methods of the production (induction or arc melting) or by the sintering of elemental powders the obtaining of homogeneous alloys, free of these phases, is not achievable.

Ti-Ni-Hf(Zr) alloys could perform reversible martensitic transformation at 100-150 °C higher than the room temperature depending on Hf content. Although the decomposition processes modifying their properties were not found in the working interval temperature, the limited ductility, poor machinability and formability restrict theirs wide practical applications. As well as for Cu-Al-Ni and Ni-Al, the powder metallurgy (PM) is thought to be good alternative method for their production and allowing skip over the stages of the shaping parts. Usually the PM production of Ni-Ti-based alloys from elemental components is accompanying with the precipitating of extra phases such as Ti_2Ni, Ni_4Ti_3, Ni_3Ti [1], and oxide $Ti_4Ni_2O_x$ [2]. Therefore the using of pre-alloyed powders looks as preferable way for PM processing.

It is the reason why the pre-alloyed spark erosion (SE) powders of Ti-Ni-Hf, Ni-Al and Cu-Al-Ni-Ti-Cr obtained in liquid argon were used [3, 4, 5]. Spark erosion is probably the most versatile technique available for the producing powders of metals, alloys, compounds with the diameters of particles from a few nm to sever-

* monag@imp.kiev.ua

al dozen μm. Using liquid argon as working liquid, one can obtain the powders from pre-alloyed material with a given composition, which is vitally important for functional material like SMA, free from large quantities of oxides.

The operation with pre-alloyed powders has unambiguous feedback caused by the peculiarities of the mechanism of powder sintering. The combustion sintering passing through the eutectic reactions or consumption the heat of formation of intermetallic compounds, promoting the sintering of elemental powders, is not available anymore. The mechanism of solid state diffusion sintering between the different powders particles of the same composition presumes the long term ageing. The precipitation processes are superimposed on the sintering processes during the annealing causing a decomposition of alloys with the formation of extra phases. Therefore the spark plasma sintering (SPS) method looks as a promising alternative of the conventional sintering method of pre-alloyed powders.

SPS method is express method allowing the sintering powders within several minutes in vacuum or inert gas atmosphere. It employs simultaneously the relatively high pressure, high temperature of sintering and heavy current passing through the samples that destroys the oxidation film on the powder surface providing good sintering. The method is very informative. It gives "on line" the information about the progress of the compacting, temperature interval of degassing and softening of the materials.

The goal of this work was to preliminary study the applicability of SPS method for the rapid sintering of pre-alloyed SE powders of Ti-Ni-Hf, Ni-Al and Cu-Al-Ni-Ti-Cr shape memory alloys.

2. EXPERIMENTAL PROCEDURES

2.1 Spark erosion powder preparation

Commercially pure Ti, Ni, Cu and Hf and Zr (99.9%) were used for the alloys production by the induction melting. The rods of Ni49.87-Ti40.25- Hf9.44-Zr0.30-Cu0.14at.% and Cu-13.01Al-3.91Ni-0.37Ti-0.24Crwt.% with a diameter of 6 mm was produced by AMT (Belgium). Alloy with a nominal composition Ni63Al37 arc melted and molded into bars with a diameter of 4 mm and the length of 12 cm. Part of the rods were used as electrodes for SE apparatus and the remaining were broken at 3-4 mm pieces (granules) and were used to obtain powder by spark erosion method.

The general principle of the spark-erosion processing was described in details in [3, 6] and involves the application of a heavy current between two electrodes and a lot of pieces (granules) that prepared from the pre-alloyed material both being immersed in liquid argon inside a container (Fig. 1). The key idea of the method is the melting (evaporation) of the material by the electric discharge with a duration of 5-100 μsec with subsequent quenching of molten droplets in liquid argon *in situ*. After spark erosion treatment of 100 g of granules of master alloys about 40÷70 g of powder was received depending on the material composition. In order to prevent eventual explosion of finest particles of powders they were kept in a vessel with liquid argon during the day until all argon was evaporated followed by were passivated in hexane. Then the powders were sieved and divided into three fractions: the size of less than 128 and more than 63 μm, less than 63 and more than 32 μm and less than 32 μm, designated hereinafter as 63/125, 32/63 and <32 respectively.

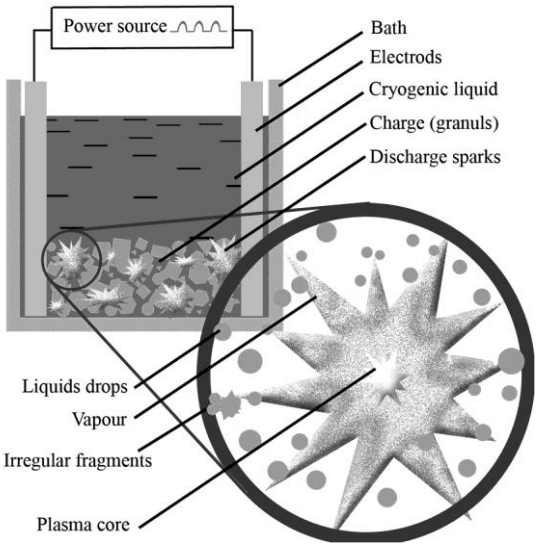

Fig. 1 – Principal scheme of the spark erosion process illustrating the formation mechanisms of micron sized and nano-sized particles during spark erosion processing

Morphology studies of spark erosion powders of all compositions have shown that micron sized particles have usually round shape (Fig. 2*a*). Nano-sized particles form the agglomerates, which cover the surface of micron sized particles (Fig. 2*a*, *b*).

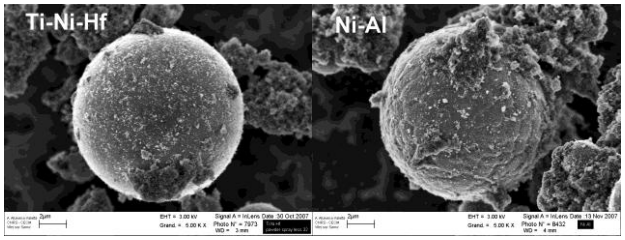

a

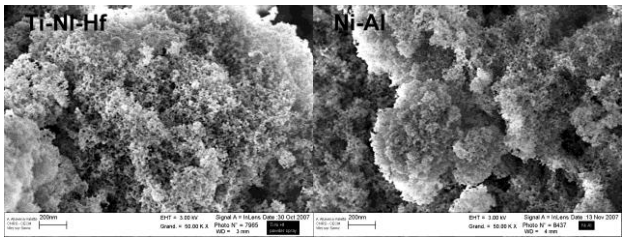

b

Fig. 2 – Morphology of micron sized (*a*) and nano- sized (*b*) particles of spark erosion powders

2.2 Spark plasma sintering processing

Fig. 3 shows the main components of the SPS apparatus (DR.SINTER® LAB Series, Metal Processing Systems, Inc. Japan). A 50 kN uniaxial press provides

a mechanical load through the die plungers for densification. Simultaneously an AC power supply applies an alternating current through the sample placed in the graphite die. About 1 g of powder was preliminary slightly compacted in the die. A graphite paper was put between the sample and the graphite plungers. Then the die was placed inside the working chamber of the

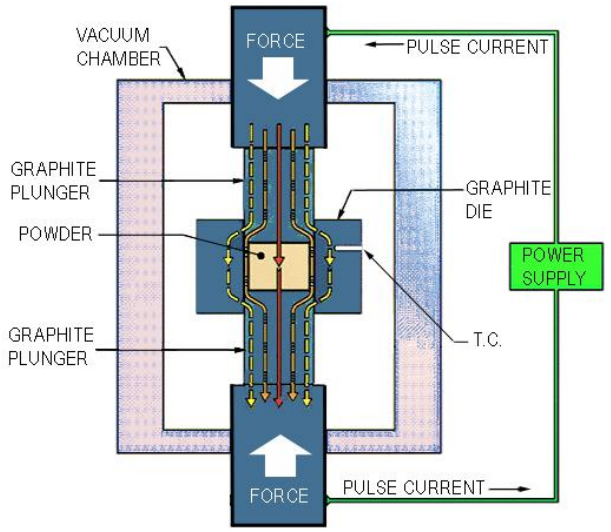

Fig. 3 – A general scheme of spark plasma sintering apparatus

apparatus and the system was evacuated. To avoid overheating of the sample the heating rate was no more 350°C/min. Maximum applied uniaxial pressure was 99.5 MPa. Temperatures of the samples during the sintering were measured by a sheathed thermocouple, which was inserted into a small hole in one side of the graphite mold, as illustrated on Fig. 3. The temperature, vacuum in the chamber, current applied force, shrinkage displacements of the powder compacts, voltage and current were recorded during the processing.

The electric current provides a rapid Joule heating in the compact die-sample system. The ramping experiment is initiated with the heating by the application of continuously increasing electric current together with

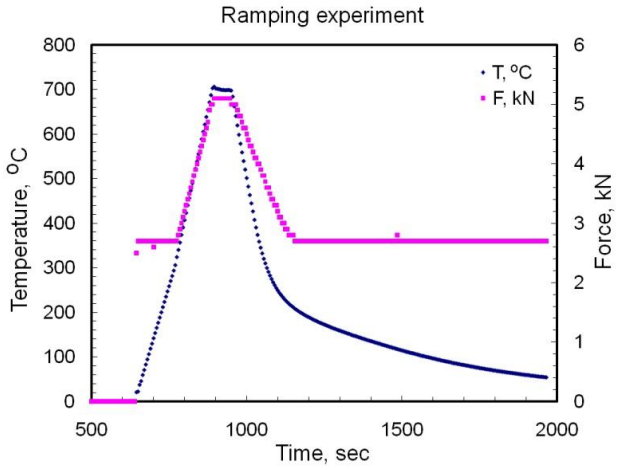

Fig. 4 – Typical program of sintering (T_{SINT} = 1000 °C; t_S=1 min)

the continuously increasing pressure. When the temperature get to preliminary setting temperature of sintering (T_{SINT}) a set constant value of the electric current was applied for a given time, hereafter indicated as sintering time (t_S). After that, the sample was unloaded, cooled and removed from the die. Temperatures of sintering were chosen according to the assessed data of the decomposition, oxidation and others processes carrying out in material. A typical program of the sintering is shown on Fig. 4. The performed programs of sintering are listed in Table 1. As a result of sintering a sintered compacts with a diameter of 8 mm and height of 4-6 mm were obtained.

Table 1 – The regimes of SPS treatment; F – applied force, HR – heating rate, d – shrinking displacement. MT means that sharp inflection of the shrinkage displacement curve (martensitic transformation) has been observed upon the cooling

Regime	T_{SINT}, °C	t_S, min	F, kN	HR, °C/min	d, mm	Remark
			Cu-Al-Ni			
CAN-1000-1	1000	1		330	1.60	Melted, 32/63
CAN-700-1	700	1		280	1.97	MT, 32/63
CAN-650-1	650	1		160	1.72	MT, 32/63
CAN-600-1	600	1	5	150	1.72	MT, 32/63
CAN-480-1	480	1		96	1.52	32/63
CAN-440-1	440	1		88	1.07	32/63
CAN-390-1	390	1		65	1.05	MT?, 32/63
			Ni-Al			
NA-400-10	400	10		200	0.22	32/63
NA-500-10	500	10		250	0.24	32/63
NA-850-10	850	10		212	0.87	MT, 32/63
NA-850-4s	850	4.5	5	212	0.86	MT, 32/63
NA-900-2	900	2		225	0.92	MT, 32/63
NA-850-4b	850	4.5		212	1.40	MT, 65/125
NA-1000-1H	1000	1		250	1.53	MT, 65/125
			Ti-Ni-Hf			
TNH-500-0	530	0	2.5	100	0.29	<32
TNH-1000-2	980	2		100	1.20	<32
TNH-860-1H	860	1	5	250	1.19	MT, 32/63
TNH-1000-1H	1000	1		200	1.42	MT, 32/63

2.3 Methods of the specimens characterization

XRD study of the compacts were carried out at room temperature by the Debye-Sherrer method with a $CoK\alpha_{1,2}$ radiation. Instrument Philips PW1830 with Multi-Purpose XRD Diffraction System from PANalytical was used.

The morphology and microstructure of the sintered samples were analyzed by LEO 1530 instrument equipped by PGT PRISM 2000 (Ge) spectrometer without the references standards. Detail composition study were carried out with JSM-6490LV(Jeol) and JAMP-9500F (Jeol) both equipped with EDX spectrometer INCA PentaFETx3 (Oxford Instruments).

3. RESULTS AND DISCUSSION

3.1 SPS process

Fig. 5 illustrates the shrinkage displacement of the powder compacts and gas pressure in the chamber during processing. For all kinds of powders the first stage of the sample shrinking was accompanied with the dramatic vacuum fall obviously related with the plungers'

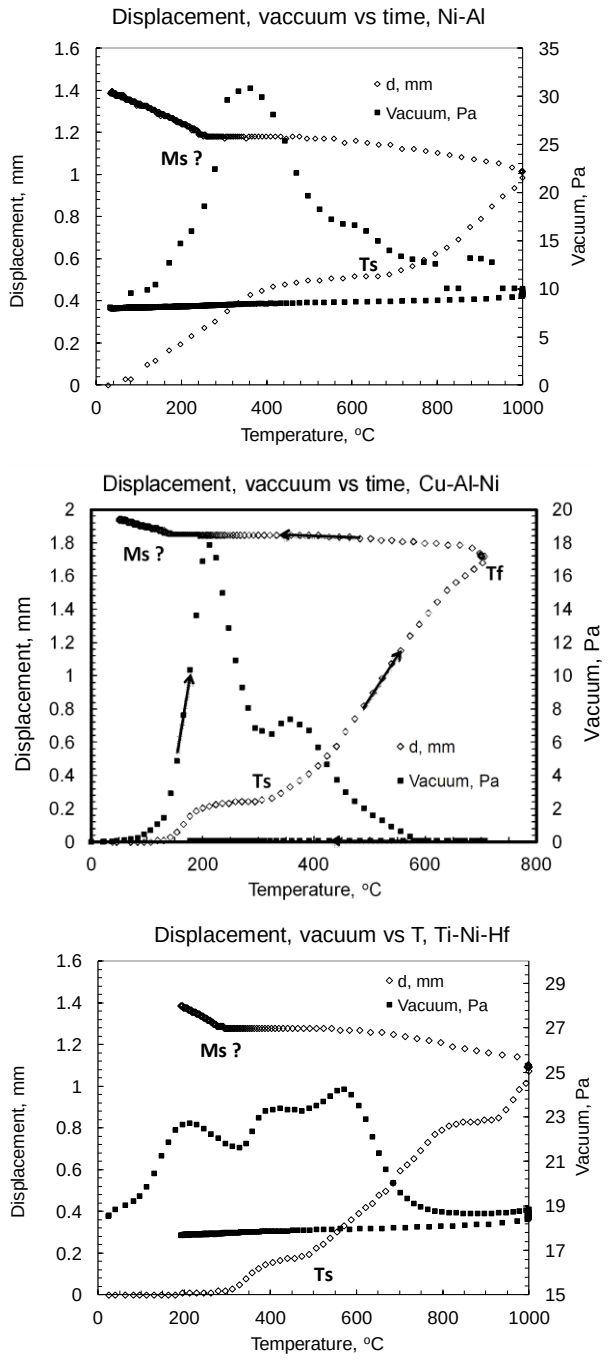

Fig. 5 – Shrinkage displacement of the specimens and gas pressure in the chamber vs. temperature. Programs NA-1000-1, CAN-700-1 and TNH-1000-1H respectively

motion. At the same time second shrinkage displacement starting at higher temperature seems to be true sintering of the particles. The temperature of the first (T_1) and second (T_S) shrinkage displacement upon the heating depends on the kind of powder. In case of Ti-Ni-Hf powder there was third interval too.

Table 2 – Temperature intervals of shrinkage displacement

Material	$T_{1\ start}$	$T_{1finish}$	$T_{S\ start}$	$T_{S\ finish}$	$T_{3\ start}$	$T_{3\ finish}$
			°C			
Cu-Al-Ni	120	250	300	>700		
Ni-Al	50	400	600-650	>1000		
Ti-Ni-Hf	300	425	475	850	910	>1000

Temperature intervals of sintering are listed in Table 2.

First sintering interval contributes about 15 %, 30-40 % and 8-15 % of the total displacement for Cu-Al-Ni, Ni-Al and Ti-Ni-Hf powders respectively. The value of contribution depends on the sizes of powders particles. The more the diameters of particle sizes, the more this contribution. It is evident that the effect of preliminary compacting (before the processing) is the less, the more the particles size. Thus one can assume that this first interval seems to be connected with the mechanical compressing and re-arrangement of powder mainly and only partial welding. It accompanied by the emission of gas (air), which is kept between the particles and squeezed out by plungers' motion. Other processes also contribute the gas emission. It could be hexane and/or water desorption (vacuum peak at about 200 °C on Ti-Ni-Hf chart on Fig. 4), collapse of porous in particles and the chemical reactions realizing the excessive gas(es). Some of the possible reactions will be discussed below.

It is seen also from Table 1 that the more the diameters of particle sizes (denoted in field "Remark" of Table 1 like 32/63 – min and max sizes of particles in powder fraction), the more total shrinkage of the compact. Thus the second and third sintering interval doesn't practically depend on the particles size. The diffusion controlled processes, promoting high temperature plasticity of the materials, such as precipitation of extra phases, decomposition, disordering contribute the shrinkage displacement effect during the successive heating.

It is interesting also that upon the cooling the extra shrinkage appeared, which was displaying as sharp inflection on the shrinkage displacement curve (M_s on Fig. 4, MT in Table 1). Because the position of sharp inflection correlate with the martensitic start point of the respective powder, on can assume that this extra compacting relates with the martensitic transformation stimulated by the external uniaxial pressure of the plungers.

Mostly powders, even sintered at relatively low temperatures were mechanically stable. Although special mechanical test were not carried out the compacts were etched and polished like bulk material. Only exclusion was Ni-Al compacts sintered according the program NA-400-10 and NA-500-10. It is easy seen from Table 2 that temperature of sintering (400 and 500°C) were below second sintering interval, thus confirms the assumption that after first interval the specimens were mechanically compacted only. Contrary Cu-Al-Ni powder sintered at 390°C (well above T_S and start temperature of α precipitation) was fairly good. However the best quality of the samples was found for the compacts sintered at higher temperatures within the interval 650-1000 °C depending on the composition of powder.

3.2 SEM investigation

SEM investigation confirmed that after the first stage of sintering only initial welding and partial compacting appeared. The particles remained mainly non-deformed with the typical round shape of SE powders (Fig. 5*a*). Contrary, the particles after the second stage of sintering were gathered tight and have been deformed (Fig. 5*b*). EDS microanalysis has shown it is not possible

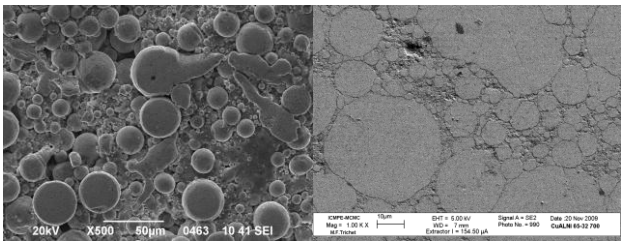

a *b*

Fig. 6 – SE images of Cu-Al-Ni powder after the compacting programs CAN-390-1 (*a*) and CAN-700-1 (*b*)

avoid the decomposition processes during SPS processing even if the very short time of sintering was used. Typical for each of powders under investigation extra

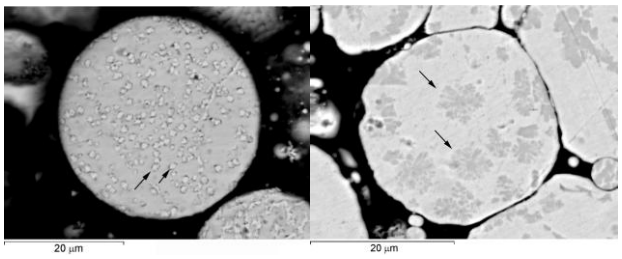

a *b*

Fig. 7 – SE images of Cu-Al-Ni powder after the compacting programs: (*a*) CAN-390-1 (arrows indicate α phases) and (*b*) CAN-700-1 ((arrows indicate γ_1 phases)

phases were found. The type of precipitates depends on the temperature of sintering mainly. γ_1 or α-phase or both of them were found in the compacts of Cu-Al-Ni after different sintering programs (Fig. 7). The X-ray mapping analyses made for the compacts sintered according to the programs CAN-700-1 and CAN-650-1 revealed the redistribution of the alloying elements (Fig. 8). Two phases are well recognized inside the particles: matrix phase and precipitated phase sized of several microns with the composition close to Cu_9Al_4. Superficial and interspaces phases between the particles are also well recognized. The redistribution of the elements is caused by two different mechanisms of the powder formation by spark erosion: micron sized particles coming from liquid phase and nano-sized particles coming from vapor of species through the condensation [3]. Thus the phase on the surface of particles (superficial) and the phase from the interspaces between the particles are rather the mixture of copper and aluminum oxides.

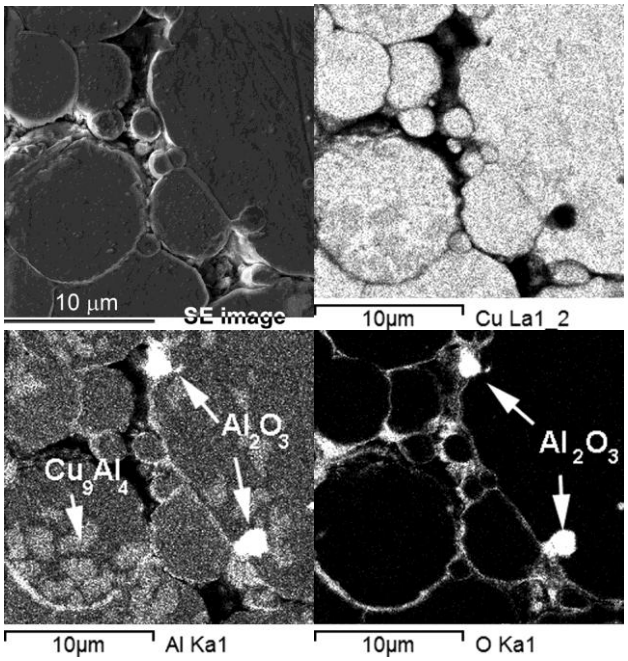

Fig. 8 – X-ray elements mapping of the Cu-Al-Ni compact sintered according to the program CAN-650-1

Enriched with Ni phase (perhaps Ni_3Al) was found in Ni-Al powder after NA-850-4s program (Fig. 9*a*). It seems to be inherited from the initial microstructure on Ni-Al SE powders described elsewhere [5]. The interspaces phase between the particles contains many small

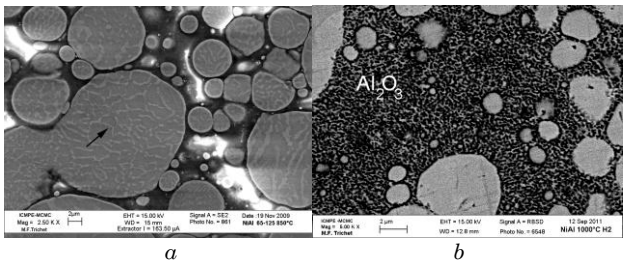

a *b*

Fig. 9 – Ni-Al powder after the program NA-850-4s; arrow indicates the enriched with Ni precipitates (*a*); morphology of interspaces' phase (presumable Al_2O_3) (*b*)

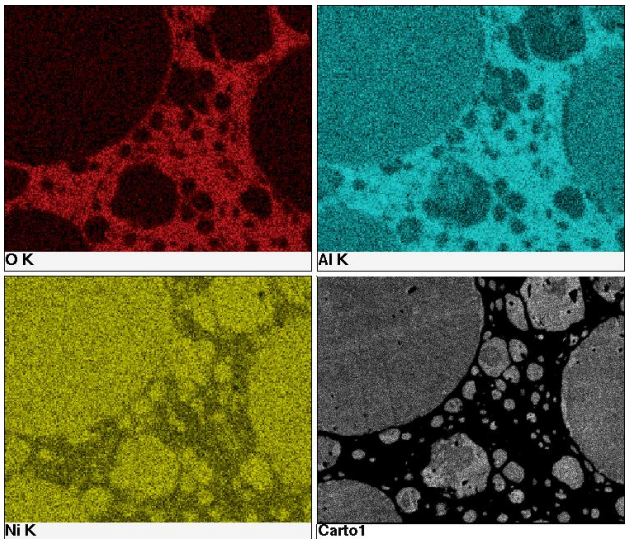

Fig. 10 – X-ray elements mapping of the Ni-Al compact sintered according to the program NA-1000-1H

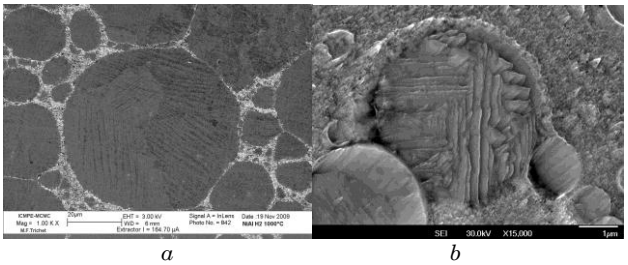

a *b*

Fig. 11 – Band (martensite) structure in recrystalized Ni-Al particles program NA-1000-1H (*a*); band structure resembling martensite in the Cu-Al-Ni particle (program CAN-700-1) (*b*)

pores (Fig. 9*b*) and consists of aluminum oxide (Fig. 10). After NA-1000-1 program some of the particles were recrystallized and banded structure resembling the martensite was also found (Fig. 11*a*). It is interesting that banded structure resembling the martensite was also found in Cu-Al-Ni compacts after etching by Ar+ ions beam (Fig. 11*b*).

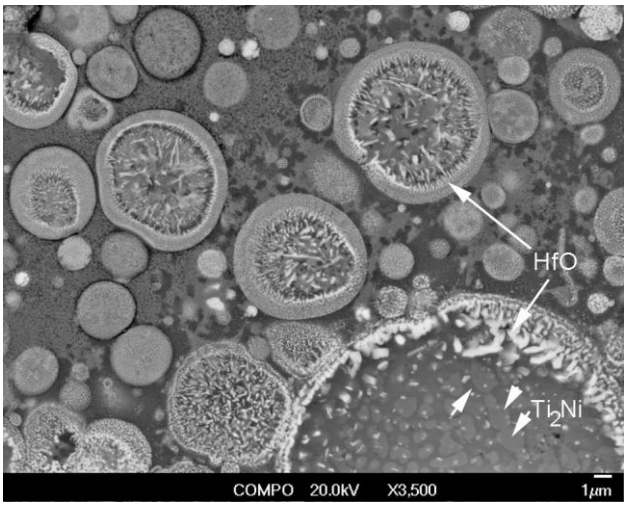

Fig. 12 – Ti-Ni-Hf powder after the compacting programs TNH-1000-2. Bright spots and needles are the enriched with Hf and oxygen phase

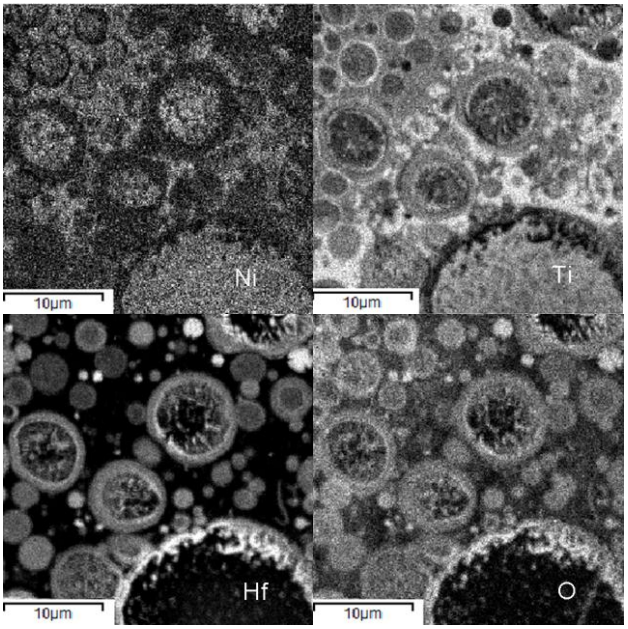

Fig. 13 – X-ray elements mapping of the Ti-Ni-Hf powder sintered according to the program TNH-1000-2

In addition to the enriched with Ni phase (seems to be Ti_2Ni), a lot of enriched with Hf and oxygen precipitates (with the composition close to HfO_2) were found into Ti-Ni-Hf powders particles as well as on their boundaries (Fig. 12). Dramatic redistribution of Ni and Ti was found in interspaces phase between the microns sized particles (Fig. 13) while Hf is concentrated in microns particles.

3.3 XRD investigation

XRD study confirmed the results of SEM investigation. B2, both martensitic 2H and 18R phases, γ_1 and α-phase or both of them are the main phases in the Cu-Al-Ni compacts after sintering while in the powder only 2H and B2 were found. In addition, instead of CuO oxide in powder some noticeable quantity of Cu_2O oxide was found in the sintered compacts.

Although the sintering time was rather short (1-4 min) it does not prevent the formation of the Ni_5Al_3 phase below 900 °C. Ni_3Al phase has formed in the samples sintered at higher temperatures; the lowest amount of this phase was found for Ni-Al powders treated according to the program NA-1000-1. Some minute peaks observed in sintered compacts as well as in powder could be considered as belonging to Al_2O_3 phase.

In addition to the peaks of B2, Ti_2Ni and B19' (martensite) phases, which are typical for powders' and massive material spectra, a lot of HfO_2 peaks were found in Ti-Ni-Hf compacts.

3.4 Effect of nano- fraction on sintering mechanism

The results obtained shown that the spark plasma sintering method allows sinter the particles of multi components alloys during extremely short time. According to Fig. 4 the stay of powders above relatively "safety" temperature of 300 °C (from decompositions and other diffusion controlled processes point of view) was no more 400 sec. Moreover Cu-Al-Ni and Ti-Ni-Hf powders were sintered during 1 min even at 390 and 500 °C respectively. These temperatures are too low to provide solid state diffusion controlled sintering mechanism. Fig. 12 allows estimating the role of elements diffusion in mechanism of sintering – the spatial migration of Ti, Ni, Hf and O atoms is about 1÷2 mkm. At first sight it is more than enough to make available good adhesion between the particles and thus sintering mechanism. However clearly observed boundaries between the particles even in well sintered compacts (Figures 7*b*, 11*a*, 12) refute this statement.

It is considered that applying electrical current during the spark plasma sintering produces a cleansing plasma effect on the surface of the particles [7-10], electron wind effect (electromigration) [11], an increase in point defect [12], a decrease in the activation of migration of the defects. All of these effects can lead to sintering enhancement [13]. In case of spark erosion powder the effect of nano-sized fraction of powders should be taken into account. The nano-fraction of powders, filling the interspaces between the micron sized particles, can enhance the sintering through the highly exothermic reactions between the different species in nano- fraction producing cohesive, coupling skeleton from the different type of oxides and alloy.

One of the possible reactions in Ti-Ni-Zr and Ti-Ni-Hf nano- fraction of spark erosion powders was proposed in [14, 15]. It is highly exothermic redox reaction between NiO and TiO oxides: $TiO + NiO \rightarrow TiO_2 + Ni$, which appears in nano powders. As it is seen from Fig. 12, 13 very reactive Hf can modify the path of reaction in case of micron sized particles however with

the same result – the formation of Hf and Ti oxides. Also the redox reaction can take place in Cu-Al-Ni nano- powders as was discussed in [16]. In that case two possible type of reaction are possible:

1) – $4CuO + 2Al + 1/2O \rightarrow 2Cu_2O + Al_2O_3$ and

2) – $2Al + 6CuO = 3Cu_2O + Al_2O_3$. Both of reactions are highly exothermic resulting in the mixture of oxides binding the micron sized particles. It is not clear the possible mechanism (if any) of oxide formation in Ni-Al powder because of traces of Al_2O_3 oxide was found already in powder. However this oxide is a dominant phase filling the interspaces between the micron sized particles as well produced from nano- fraction and one can expect that similar (may be more complex) reaction is responsible for the sintering mechanism.

As a result of above mentioned reactions complex composite structure is formed from the oxides and other products with embedded micron sized particles. Thus the role of the nano- spark erosion powders seems to be double: from one hand the presence of nano- powders promotes the sintering, from the other one it is hard to expect good shape memory characteristics from such complex composite (alloy + oxides).

4. CONCLUSIONS

The compacts of Ni49.87-Ti40.25-Hf9.44-Zr0.3-Cu0.14at.%, Cu-13.01Al-3.91Ni-0.37Ti-0.24Crwt.% and Ni63Al37 shape memory alloys were elaborated by the spark plasma sintering method from the micron, submicron and nano- sized particles prepared by spark-erosion method in liquid argon from preliminary melted master alloys.

Although the strongly shrinkage displacement has been observed already at relatively low temperature (< 300-400 °C), true sintering has appeared in the compacts sintered at higher temperatures.

Rapid sintering prevents the intensive grain growth in most cases and provides the inheritance of most microstructure peculiarities of as-received powder by the sintered material. Even the sintering time was rather short (1-10 min) it does not prevent the precipitation of extra phases.

Highly exothermic reactions between nano- fractions (NiO/TiO/Hf), (CuO/Al) can promote from one hand the sintering, from other hand the oxidation processes during the SPS sintering.

The martensitic transformation in most of the sintered compacts has been clearly indicated during the cooling in spark-plasma apparatus; martensitic structure was confirmed by SEM and XRD study.

AKNOWLEDGEMENTS

The authors are grateful to CNRS PICS-3717, STCU-3520 and ECONET projects for the supporting of this work.

REFERENCES

1. G.E. Monastyrsky, J. Van Humbeeck, V.I. Kolomytsev, Y.N. Koval, *Intermetallics* **10**, 613 (2002).
2. M. Nishida, C.M. Wayman, T. Honma, *Metall. Trans. A* **17**, 1505 (1986).
3. G.E. Monastyrsky, P.A. Yakovenko, V.I. Kolomytsev, Yu.N. Koval, A.A. Shcherba, R. Portier, *Mater. Sci. Eng. A* **481-482**, 643 (2008).
4. G.E. Monastyrsky, P. Ochin, G.Y. Wang, A.V. Gilchuk, V.I. Kolomytsev, Yu.N. Koval, V.O. Tinkov, A.A. Shcherba, S.M. Zaharchenko, *Chem. Met. Alloys* **4**, 126 (2011).
5. G.E. Monastyrsky, V.V. Odnosum, V.I. Kolomitsev, Yu.N. Koval, P. Ochin, R. Portier, A.A. Shcherba, S.N. Zaharchenko, *Metallofiz. Novejsh. Tehnol.* **30**, 761 (2008).
6. A.E. Berkowitz, M.F. Hansen, F.T. Parker, K.S. Vecchio, F.E. Spada, E.J. Lavernia, R. Rodriguez, *J. Magn. Magn. Mater.* **254-255,** 1 (2003).
7. M. Tokita, *Mater. Sci. Forum* **308-311**, 83 (1999).
8. Z. Shen, M. Johnsson, Z. Zhao, M. Nygren, *J. Amer. Ceram. Soc.* **85,** 1921 (2002).
9. M. Omori, *Mater. Sci. Eng. A* **287**, 183 (2000).
10. D. Zhang, Z. Fu, R. Yuan and J. Guo, *Multiphased Ceramic Materials* (Ed. W.H. Tuan and J.K. Guo) (Springer: Berlin: 2004).
11. H.B. Huntington, *Diffusion in Solids* (Ed. A.S. Nowick and J.J. Burton (Academic Press: New York: 1975).
12. P. Asoka-Kumar, M. Alatalo, V.J. Gosh, A.C. Kruseman, B. Nielson, K.G. Lynn, *Phys. Rev. Lett.* **77**, 2097 (1996).
13. Z.A. Munir, U. Anselmi-Tamburini, *J. Mater. Sci.* **41**, 763 (2006).
14. O.M. Ivanova, M.I. Danilenko, G.E. Monastyrsky, V.I. Kolomytsev, Yu.N. Koval, A.A. Scsherba, S.M. Zaharchenko, R. Portier, *Metallofiz. Novejsh. Tehnol.* **31**, 603 (2009).
15. G.E. Monastyrsky, V.I. Kolomytsev, Yu.N. Koval, P. Ochin, G. Vang, O. M. Ivanova, N.I. Danilenko, *Metallofiz. Novejsh. Tehnol.* **33**, 289 (2011).
16. P. Ochin, A.Yu. Pasko, G.E. Monastyrsky, A.V. Gilchuk, V.I. Kolomytsev, Yu.N. Koval, R. Portier, Spark plasma sintering of Cu-Al-Ni shape memory alloy, to be published in *J. Alloy Compd*.